IEEE Access
Multidisciplinary | Rapid Review | Open Access Journal

Received June 12, 2018, accepted July 11, 2018, date of publication July 25, 2018, date of current version August 20, 2018.

Digital Object Identifier 10.1109/ACCESS.2018.2859750

A Joint Distribution-Based Testability Metric Estimation Model for Unreliable Tests

XUERONG YE[1], (Senior Member, IEEE), CEN CHEN[1], (Student Member, IEEE), MYEONGSU KANG[2], (Member, IEEE), GUOFU ZHAI[1], (Member, IEEE), AND MICHAEL PECHT[1], (Fellow, IEEE)

[1]Department of Electrical Engineering, Harbin Institute of Technology, Harbin 150001, China
[2]Center for Advanced Life Cycle Engineering, University of Maryland at College Park, College Park, MD 20742, USA

Corresponding author: Cen Chen (macchan_hit@sina.com)

This work was supported in part by the National Key Research and Development Program of China under Grant 2017YFB1300800, in part by the National Natural Science Foundation of China under Grant 61671172, and in part by the China Scholarship Council under Grant 201706120196.

ABSTRACT The selection of tests required to make complex systems testable is a fundamental of system-level fault diagnosis. To evaluate the test selection, testability metric estimation (TME) is required. The influence of unreliable (imperfect) tests, whose outcomes are non-deterministic due to unstable environmental conditions, test equipment errors, and component tolerances, should be considered for accurate TME. Previously, researchers considered a TME model using a Bernoulli distribution with the assumption that the variations of different test outcomes are independent. However, this assumption is not always true. To address the issue, a joint distribution-based TME model was developed derived from the copula function to quantify the influence of dependent outcomes of unreliable tests. The efficacy of the developed TME model was verified with a linear voltage divider and a negative feedback circuit.

INDEX TERMS Copula theory, fault diagnosis, testability metric estimation, and unreliable tests.

I. INTRODUCTION

With the rapid development of manufacturing techniques, large and complex systems can be designed and deployed in critical fields such as aircraft, spacecraft, and nuclear power plants [1]. To ensure that complex systems run efficiently, the testability of systems must be considered. Thus, a series of tests, as well as corresponding physical sensors or interfaces, should be clarified during the design phase. These tests provide the original information for the system, which is fundamental to system-level fault diagnosis, prognosis, and health management [2], [3]. The selection of tests can significantly influence the diagnostic resolution and life cycle maintenance costs [4]–[6]. To evaluate the potential diagnostic resolution of selected tests in the design phase, some testability metrics (TMs) are needed, such as fault detection rate (FDR), fault isolation rate (FIR), and false alarm rate (FAR).

To realize testability metric estimation (TME) for a given test subset, a fault/test dependency model, which describes the relationship between faults and tests, should be established. Various dependency modeling methods have been developed, which can be categorized into two groups: digraph-based methods [7]–[11] and simulation-based methods [12], [13]. Digraph-based methods, which have been mainly used for large-scale modular systems, establish a dependency model by extracting fault propagation characteristics from the functional block diagram of the system. The well-known digraph-based methods include the information flow method [8], the multi-signal flow graph method [9], and the quantitative directed graph method [10]. Simulation-based methods establish a dependency model by acquiring fault effects from system simulation. Due to the development of electronic design automation (EDA) techniques, simulation-based methods have been developed rapidly in small-scale circuit systems [14]–[18]. As a result of these modeling methods, a dependency matrix (D-matrix) can be derived. Then, TME for ideal tests can be realized using Boolean operations on the derived D-matrix.

In the above studies, test outcomes are assumed to be deterministic under each given fault state. However, test outcomes in real systems are non-deterministic due to various uncertainty factors, such as sensor errors, electromagnetic interference, component tolerances, and environmental conditions [6]. The tests whose outcomes are non-deterministic are called unreliable tests or imperfect tests [6], [19]. The existence of unreliable tests does not affect the ideal

value of each test outcome under given fault states. However, the test outcome will vary at a certain range near the ideal value, and the diagnostic performance of a given test subset can also be influenced by unreliable tests. Hence, several studies have been conducted to quantify the influence of unreliable tests [6], [20]–[25]. Nachlas *et al.* [20] presented unreliable test outcomes in the form of false positives and false negatives, and the priori probabilities of incorrect test outcomes were assumed from historical data. The influence of unreliable tests was then evaluated in terms of incorrect repairs cost. Raghavan et al. [21] described variations of unreliable tests using the detection/false alarm probability pair. This probability pair was also used as information to decide the test sequencing for fast fault diagnosis. Ying *et al.* [22] and Ruan *et al.* [23] also used such probability pairs as the posteriori probabilities in the hidden Markov model to solve dynamic single-fault diagnosis and multiple-fault diagnosis, respectively.

Although different methods have been used to represent unreliable tests, they all regard each test outcome as a specific Bernoulli distribution instead of a deterministic binary in the D-matrix. Following the same idea, Zhang *et al.* [6] first proposed a Bernoulli distribution-based TME model, which is also the only TME model for unreliable tests up to now. The influence of unreliable tests was quantified using a probability that is the product of a series of probabilities deriving from Bernoulli distributions of test outcomes. This model was further adopted to solve the test selection problem [6], [25], the testability growth problem [26], [27], and the testability evaluation problem [28].

In the above Bernoulli distribution-based TME model, test outcomes were assumed to be independent random variables under given fault states. This assumption indicates that knowing the outcome of one test does not change the probability of the outcome of any other test. However, this is not always true in the real world. For example, if temperatures in two terminals of a shaft are tested, these two temperatures should be dependent since the environmental temperature causes their variations at the same time. To the best of the authors' knowledge, no paper has considered such dependency among test outcomes in TME problem.

In view of the above, the scope of this study mainly focuses on addressing issues of TME with unreliable tests, which assumes that the specific dependency model has been given already. The main contributions of this study are to prove dependent relationships among outcomes of unreliable tests and to develop a joint distribution-based TME model to address the dependency among test outcomes. In contrast with Bernoulli distribution, which is a univariate distribution, the joint distribution refers to the distribution of multivariables. It regards all test outcomes as a whole, thus the dependent relationships that were ignored in the Bernoulli distribution-based TME model can be considered. Among various joint distributions, a specific joint distribution constructed by the copula theory was also derived in the TME model, because of its high adaptability of variables and simplicity of construction.

The rest of this paper is organized as follows. Section II presents the dependent relationships among test outcomes by enumerating several examples and establishing a qualitative model of the test outcome. Section III describes the joint distribution-based TME model. In addition, a copula joint distribution-based TME model is provided. In Section IV, two examples are used to demonstrate the construction process of the developed TME model and validate its efficacy. Section V summarizes the main contributions.

II. DEPENDENT RELATIONSHIPS AMONG TEST OUTCOMES

Due to the existence of unreliable tests, each test outcome can be treated as a random variable, and uncertainty factors are treated as input variables. Previous studies treated test outcomes as independent random variables, which means knowing the outcome of one specific test does not change the probability of the outcome of any other test. However, this situation is impractical. To prove this point of view, several examples that show the incongruence of an independent relationship between two test outcomes are presented. Then, a qualitative model of the test outcomes is established, which explains the relationship between the test outcomes and uncertainty factors and generalizes the causes of dependent relationships among test outcomes.

A. OUTCOMES OF TWO TESTS DERIVED FROM THE SAME TEST EQUIPMENT

For a complex system, several tests related to the same type of signal can be conducted using the same test equipment. For example, if several voltage-related tests are needed in a circuit, only one oscilloscope or one data acquisition (DAQ) card is enough to monitor all these voltage signals. The test equipment introduces uncertainty to the test outcomes. Since the same test equipment is used to conduct different tests, the outcome shifts of these tests should be the same.

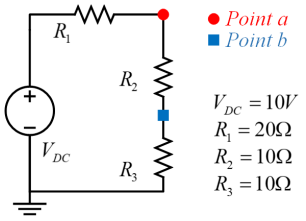

FIGURE 1. Example circuit to show the influence of the dependency between two test outcomes.

Using the electronic circuit in Fig. 1 as an example, the voltage test of physical points a and b is defined as two tests, which are referred to as t_a and t_b, respectively. According to electronic theory, the ideal values t_{a0} and t_{b0}

can be derived as:

$$\begin{cases} t_{a0} = V_{DC} \cdot (R_2 + R_3) / (R_1 + R_2 + R_3) \\ t_{b0} = V_{DC} \cdot R_3 / (R_1 + R_2 + R_3) \end{cases} \quad (1)$$

For voltage measurement, a reference voltage is required in the test equipment (oscilloscope or DAQ card). The reference voltage may fluctuate slightly, which can further affect the outcomes of these two tests. Thus, the outcomes of the two tests can be modified as:

$$\begin{cases} t_a = t_{a0} + \delta_s \\ t_b = t_{b0} + \delta_s \end{cases} \quad (2)$$

where δ_s denotes the error introduced by the reference voltage in the test equipment. In this case, variations of both test outcomes are caused by the fluctuation of the reference voltage. δ_s is the same in both equations. If t_a is observed to be higher than t_{a0}, then the observation of t_b must be higher than t_{b0}. Since the observation of t_a determines the probability of the observation of t_b, the two test outcomes do not satisfy the independent random variables assumption.

B. OUTCOMES OF TWO TESTS RELATED TO THE SAME COMPONENTS

In the complex system, the outcomes of different tests can also be influenced by the same components. Tolerance can cause the parameters of these components to vary, which in turn can result in variations of different test outcomes. Taking the same circuit in Fig. 1 as an example, the resistance fluctuation of R_1 can affect both voltage tests. Considering the tolerance influence of R_1, the outcomes of the two tests should be:

$$\begin{cases} t_a = V_{DC} \cdot (R_2 + R_3) / (R_1 + \delta_c + R_2 + R_3) \\ t_b = V_{DC} \cdot R_3 / (R_1 + \delta_c + R_2 + R_3) \end{cases} \quad (3)$$

where δ_c denotes the resistance shift introduced by component tolerance. In this case, variations of these two test outcomes are only caused by δ_c. Given a specific observation of t_a, the observation of t_b will also be determined. Thus, the two test outcomes also do not satisfy the independent random variables assumption.

C. OUTCOMES OF TWO TESTS INFLUENCED BY THE TEST ENVIRONMENT

Another case is related to the test environment. During the test process, environment conditions can affect most of the test outcomes, since the environment can influence the state of the system under test (SUT). Assuming that only the voltage source is affected by temperature with a positive temperature coefficient K_T in the above circuit example, the test outcomes can be modified as:

$$\begin{cases} t_a = V_{DC} \cdot (1 + K_T \cdot \delta_T) \cdot (R_2 + R_3) / (R_1 + R_2 + R_3) \\ t_b = V_{DC} \cdot (1 + K_T \cdot \delta_T) \cdot R_3 / (R_1 + R_2 + R_3) \end{cases} \quad (4)$$

where δ_T denotes the fluctuation of environment temperature. If an observation of t_a is higher than the ideal value t_{a0}, it indicates that the environment temperature is higher than normal ($\delta_T > 0$). At the same time, it can cause the observation of t_b to be higher than t_{b0}. Again, the two test outcomes do not satisfy the independent random variable assumption.

D. GENERALIZATION OF CAUSES FOR DEPENDENCIES AMONG TEST OUTCOMES

In all of the above three cases, the test outcomes are not independent random variables. However, these cases do not fully represent this issue. In general, as long as two test outcomes are influenced by the same input variable(s), they are not independent random variables. To generalize the causes for the dependency among test outcomes, the relationship between the test outcome and uncertainty factors should be modeled.

During the test process, the principal sources of unreliable tests are the state uncertainty of the SUT, environmental uncertainty, measuring method uncertainty, and inherent uncertainty of the measurement equipment. The qualitative relationship between the test outcome t and these uncertainty factors can be expressed as follows:

$$t = T\left[\varphi(F, U), S, \delta^m\right] + \delta^e \quad (5)$$

where F denotes the system fault state, U denotes the parameters of system components or functional modules, S denotes operating environmental stress, δ^m denotes the error from the measuring method uncertainty, and δ^e denotes the error introduced by the uncertainty of measurement equipment. $\varphi()$ represents the state of the SUT, which is a function of F and U. $T()$ is the function expressing the relationship between the test outcomes and the state of the SUT. In (5), δ^e, δ^m, S, and U are uncertain, among which U is variable due to the component tolerances of the system, and S is determined by environmental factors such as temperature and humidity. The test outcomes can then be regarded as random variables due to the uncertainties that arose from δ^e, δ^m, S, and U.

Similarly, the outcomes of two specific tests t_1 and t_2 can be expressed, respectively, as:

$$\begin{cases} t_1 = T_1\left[\varphi(F, U), S, \delta_1^m\right] + \delta_1^e \\ t_2 = T_2\left[\varphi(F, U), S, \delta_2^m\right] + \delta_2^e \end{cases} \quad (6)$$

where T_1 and T_2 represent different measuring methods referring to different tests. Since these two random variables t_1 and t_2 contain the same input variables of S and U, they are mathematically dependent. Therefore, any factor that causes variations of S or U can make test outcomes be dependent random variables.

III. A JOINT DISTRIBUTION-BASED TESTABILITY METRIC ESTIMATION MODEL USING THE COPULA FUNCTION

Section II proved that test outcomes can be dependent random variables, and thus the conventional Bernoulli distribution-based TME model with the assumption of independent random variables is no longer useful. In this section, the drawbacks of the conventional model are shown using an example

first. Then the developed joint distribution-based TME model is presented to solve these drawbacks. Three of the most used TMs—FDR, FAR, and FIR—are considered. In addition, the copula function is used to construct the joint distribution in the developed model.

A. DRAWBACKS OF THE CONVENTIONAL TME MODEL

As mentioned in Section I, the Bernoulli distribution was developed in the D-matrix to consider the influence of unreliable tests. The D-matrix can be expressed as follows:

$$D_{m\times n} = \begin{array}{c} \\ ft_1 \\ ft_2 \\ \vdots \\ ft_m \end{array} \begin{array}{c} \begin{array}{cccc} t_1 & t_2 & \cdots & t_n \end{array} \\ \begin{bmatrix} r_{11} & r_{12} & \cdots & r_{1n} \\ r_{21} & r_{22} & \cdots & r_{2n} \\ \vdots & \vdots & \ddots & \vdots \\ r_{m1} & r_{m2} & \cdots & r_{mn} \end{bmatrix} \end{array} \tag{7}$$

where t_j and ft_i represent the j-th test and i-th fault, respectively. The element r_{ij} denotes whether t_j responds to ft_i. Let $r_{ij} = 1$ (fail) if t_j responds to ft_i, and otherwise $r_{ij} = 0$ (pass).

In the Bernoulli distribution-based TME model, the probabilistic relationship between faults and test outcomes is represented by element d_{ij}:

$$d_{ij} = r_{ij} \cdot Pd_{ij} + (1 - r_{ij}) \cdot Pf_{ij} \tag{8}$$

where Pd_{ij} and Pf_{ij} refer to the correct detection probability and the false-alarm probability of t_j for ft_i, respectively [21]. Hence, d_{ij} can indicate the response probability of t_j when ft_i occurs. The estimation of FDR and FIR with unreliable tests can be expressed as follows [6]:

$$PD_i = 1 - \prod_{j=1}^{n} \left(1 - d_{ij}\right) \tag{9}$$

$$PI_i = \prod_{k=1,k\neq i}^{m} \left(1 - \prod_{j=1}^{n} \left[(1 - d_{ij})(1 - d_{kj}) + d_{ij}d_{kj}\right]\right) \tag{10}$$

where n is the total test amount, m is the total fault amount, and PD_i and PI_i refer to the FDR and FIR of ft_i, respectively.

To set up (9) and (10), the test outcomes must be assumed to be independent random variables based on the probability theory. Thus, the conventional Bernoulli distribution-based TME model cannot be applied to solve the cases wherein test outcomes are dependent.

To illustrate the dependency problem, the electronic circuit in Fig. 1 is used as an example. The resistance tolerance of R_2 is assumed to be the only uncertainty factor in this case. When R_2 fluctuates, t_a and t_b obey the normal distributions shown in Fig. 2. Assuming that the fault response criteria of the two tests are specified as $t_a < 5$ V and $t_b > 2.5$ V, respectively, then the estimated fault detection probability is $1 - (1 - 50\%) \times (1 - 50\%) = 75\%$ according to (9). However, t_a and t_b are positively correlated no matter what R_2 is, which means t_b must be lower than 2.5 V if t_a is lower than 5 V. Thus, the probability of the event that $t_a < 5$ V and $t_b > 2.5$ V should be 0%, and the expected fault detection probability should be $1 - 0\% = 100\%$.

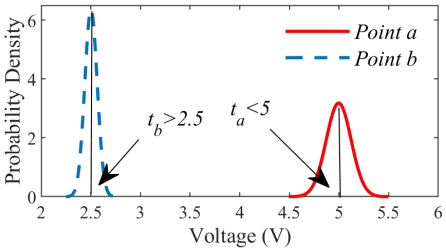

FIGURE 2. Distribution of two test outcomes.

In the example, the Bernoulli distribution-based TME model resulted in a totally incorrect fault detection probability (0%), which is far away from the expected value (100%). The example proved that the conventional TME model has a severe drawback if dependent relationships exist among test outcomes.

B. TME MODEL WITH THE JOINT DISTRIBUTION

To address the dependency among test outcomes, the joint distribution should be considered instead of Bernoulli distribution. The joint distribution of n-dimensional random variables $X = (X_1, X_2, \ldots, X_n)$ gives the probability that each random variable in X falls in any particular range. The continuous joint distribution function can be expressed as:

$$F_X(x) = P\left(\bigcap_{j=1}^{n} X_j \leq x_j\right) \tag{11}$$

where x is the particular upper limit vector of X.

This joint distribution function is the core of the developed TME model in this paper. When constructing the joint distribution, the dependency among test outcomes can be fully considered to address the drawbacks of previous models. Before estimating TMs with the joint distribution, the following notations and assumptions should be made:

1) The system faults are represented as $FT = (ft_0, ft_1, \ldots, ft_m)$, where ft_0 denotes the fault-free state.
2) The full test set (including all candidate tests) is $T = (t_1, t_2, \ldots, t_n)$, of which the outcome of each test is assumed to be a continuous variable, and the corresponding test thresholds are represented as $THR = (thr_1, thr_2, \ldots, thr_n)$.
3) Suppose ft_i occurred, if the outcome of t_j (represented as t_{ji}) is greater than the specified thr_j, then t_j is believed to have the ability to respond to ft_i, which can be expressed as $r_{ij} = 1$. Otherwise, $r_{ij} = 0$.
4) The test selection vector is defined as $S = (s_1, s_2, \ldots, s_n)$, where $s_j = 1$ if t_j is selected, otherwise $s_j = 0$.

1) FDR AND FAR ESTIMATION

For a specific fault ft_i, the equivalent condition of fault detection success is that at least one test does respond to ft_i when ft_i occurs. Thus, the FDR of ft_i is expressed as:

$$FDR(ft_i) = 1 - P\left(t_j^i \leq thr_j | j \in [1, n]\right) \tag{12}$$

where t_j^i represents the outcome of t_j when f_i occurs. Then, the FDR can be expressed using a joint distribution function as:

$$\begin{cases} FDR(ft_i) = 1 - F_X(x) \\ X = (X_1, X_2, \cdots, X_n), & X_j = t_j^i \\ x = (x_1, x_2, \cdots, x_n), & x_j = thr_j \end{cases} \tag{13}$$

where the test outcomes of f_i and the test thresholds are defined as the n-dimensional random variables X and the particular upper limit vector x of the joint distribution function, respectively.

When the test selection is considered, the upper limits of the tests that are not selected should be modified to the positive infinite ($+\infty$). Therefore, the equation can be modified as:

$$FDR(ft_i; S) = 1 - P\left(t_j^i \le thr_j | s_j = 1 \cap t_j^i \le +\infty | s_j = 0\right) \tag{14}$$

To keep the input dimension consistent, the part of $s_j = 0$ should also be reserved in the joint distribution function. Thus, an operator $\odot$ is defined to solve this issue as follows:

$$a \odot b = \begin{cases} a & b = 1 \\ +\infty & b = 0 \end{cases} \tag{15}$$

Then, the FDR with a specific test selection vector S can be represented as:

$$\begin{cases} FDR(ft_i; S) = 1 - F_X(x^*) \\ X = (X_1, X_2, \cdots, X_n), & X_j = t_j^i \\ x^* = \left(x_1^*, x_2^*, \cdots, x_n^*\right), & x_j^* = thr_j \odot s_j \end{cases} \tag{16}$$

The equivalent condition of false alarm is that at least one test incorrectly responds to the fault-free state ft_0. Thus, the FAR can be regarded as the FDR of ft_0. Then, the FAR with a specific S can be represented as:

$$\begin{cases} FAR(S) = FDR(ft_0; S) = 1 - F_X(x^*) \\ X = (X_1, X_2, \cdots, X_n), & X_j = t_j^0 \\ x^* = \left(x_1^*, x_2^*, \cdots, x_n^*\right), & x_j^* = thr_j \odot s_j \end{cases} \tag{17}$$

2) FIR ESTIMATION

For a specific ft_i, the fault isolation success must satisfy the following two conditions: (C1) the test pattern of ft_i must be unique, i.e., in the Boolean D-matrix, the row of ft_i must be different from any other row, and (C2) the test outcomes must be the same as the expected test pattern of ft_i.

Aiming at (C1), a similarity value LI_{ik} is defined to describe the diversity of test patterns between ft_i and ft_k, which is expressed as follows:

$$LI_{ik} = \prod_{j=1}^{n} \left[\left(1 - r_{ij}\right)\left(1 - r_{kj}\right) + r_{ij} r_{kj}\right] \tag{18}$$

When the test patterns of ft_i and ft_k are the same, then $LI_{ik} = 1$. Thus, (C1) can be expressed as:

$$LI_i = \prod_{k=1, k\neq i}^{m} \left(1 - LI_{ik}\right) \tag{19}$$

where $LI_i = 1$ if (C1) is satisfied.

Aiming at (C2), the probability that test outcomes are the same as the expected test pattern of ft_i can be expressed as PI_i:

$$PI_i = P\left(t_p^i \le thr_p | r_{ip} = 0 \cap t_q^i \ge thr_q | r_{iq} = 1\right) \tag{20}$$

To unify the form of input variables, an item, $(-1)^{r_{ij}}$ in (21), is added and the FIR can be expressed as:

$$FIR(ft_i) = LI_i \cdot P\left((-1)^{r_{ij}} t_j^i \le (-1)^{r_{ij}} thr_j | j \in [1, n]\right) \tag{21}$$

Then, the FIR can be expressed using a joint distribution function as:

$$\begin{cases} FIR(ft_i) == LI_i \cdot F_X(x) \\ LI_i = \prod_{k=1, k\neq i}^{m} \left(1 - \prod_{j=1}^{n} \left[\left(1 - r_{ij}\right)\left(1 - r_{kj}\right) + r_{ij} r_{kj}\right]\right) \\ X = (X_1, \quad X_2, \cdots, X_n), X_j = (-1)^{r_{ij}} t_j^i \\ x = (x_1, \quad x_2, \cdots, x_n), x_j = (-1)^{r_{ij}} thr_j \end{cases} \tag{22}$$

The FIR with a specific S can be represented as:

$$\begin{cases} FIR(ft_i; S) == LI_i^* \cdot F_X(x^*) \\ LI_i^* = \prod_{k=1, k\neq i}^{m} \left(1 - \prod_{j=1}^{n} \left[\left(1 - r_{ij}\right)\left(1 - r_{kj}\right) + r_{ij} r_{kj}\right]^{s_j}\right) \\ X = (X_1, X_2, \cdots, X_n), & X_j = (-1)^{r_{ij}} t_j^i \\ x^* = \left(x_1^*, x_2^*, \cdots, x_n^*\right), & x_j^* = (-1)^{r_{ij}} thr_j \odot s_j \end{cases} \tag{23}$$

C. COPULA THEORY IN THE JOINT DISTRIBUTION CONSTRUCTION

The copula theory is widely used to construct the joint distribution. In theory, any multivariate joint distribution can be written in terms of univariate marginal distributions and a copula function [29]. Let $H(x_1, x_2, \ldots, x_n)$ represent the joint distribution function of n-dimensional variables $X = (X_1, X_2, \ldots, X_n)$, and $F_{Xi}(x_i)$ represents the marginal distribution of the variable X_i, where $i = 1, 2, \ldots, n$. Then a given $H()$ can be expressed with a unique copula function $C()$ as follows:

$$H(x_1, x_2, \cdots, x_n) = C(F_{X1}(x_1), F_{X2}(x_2), \cdots, F_{Xn}(x_n)) \tag{24}$$

where $F_{Xi}(x_i) \in [0, 1]$, and the copula function can be regarded as an n-dimensional joint distribution function whose variables all obey uniform distribution within [0, 1]. Copula theory is interpreted to transform the original n-dimensional variables to the space of $[0, 1]^n$ via their respective marginal distribution probability, and then uses a specific function $C()$ to describe the dependency of transformed multiple random variables.

To estimate various unknown parameters in the copula function, the joint probability density function (PDF) is needed, which can be expressed as $h()$:

$$h(x) = \frac{\partial^n H}{\partial x_1 \cdots \partial x_n} = c\left(\{u_j | j \in [1, n]\}\right) \cdot \prod_{i=1}^{n} f_{Xi}(x_i; \theta_i) \tag{25}$$

where $c()$ is the copula density function; $f_{Xi}()$ is the marginal PDF of X_i; and u_i and θ_i represent the marginal distribution probability and the marginal distribution parameter of X_i, respectively. Utilizing the maximum likelihood estimation (MLE) or any other methods, the given sample data can be used to estimate unknown parameters [30]. The logarithmic likelihood function of $h(x)$ is expressed as:

$$\ln L() = \sum_{i=1}^{k} \left[\ln c\left(\left\{u_{ji} | j \in [1,n]\right\}; \theta_c\right) + \sum_{j=1}^{n} \ln f_{Xj}(x_{ji}; \theta_j) \right] \tag{26}$$

where x_{ji} is the i-th sample of X_j, u_{ji} is the corresponding marginal distribution probability of x_{ji}, and θ_c represents the dependence structure parameters of the copula function.

D. COPULA-CONSTRUCTED TME MODEL

The joint distribution-based TME model can be constructed based on the copula theory. In this model, the upper limits of unselected tests are modified as the positive infinite. In the copula function, the upper limits can be modified by setting the marginal distribution probabilities of corresponding tests to 1 as follows:

$$C\left(F_{X1}\left(x_1\right), \cdots, 1, \cdots, F_{Xn}\left(x_n\right)\right) = F_X\left(x_1, \cdots, +\infty, \cdots, x_n\right) \tag{27}$$

Then, the copula-constructed TME model is as follows:

$$\begin{cases} FDR(ft_i; S) = 1 - C\left(u_1, u_2, \cdots, u_n\right) \\ u_j = F_{Xj}\left(thr_j\right)^{s_j}, \quad X_j = t_j^i \\ i \in [0,m], \quad j \in [1,n] \end{cases} \tag{28}$$

$$\begin{cases} FIR(ft_i; S) = LI_i^* \cdot C\left(u_1, u_2, \cdots, u_n\right) \\ LI_i^* = \prod_{k=1,k\neq i}^{m} \left(1 - \prod_{j=1}^{n} \left[(1-r_{ij})(1-r_{kj}) + r_{ij}r_{kj}\right]^{s_j}\right) \\ u_j = F_{Xj}\left((-1)^{r_{ij}}\, thr_j\right)^{s_j}, \quad X_j = (-1)^{r_{ij}}\, t_j^i \\ i \in [1,m], \quad j \in [1,n] \end{cases} \tag{29}$$

Several copula functions can be used, such as Gaussian copula, t-copula, and Archimedean copulas. Due to the simple structure and the similarity to the well-known Gaussian distribution function, the Gaussian copula function is used in this paper:

$$\begin{cases} C(u_1, \cdots, u_n; \theta_c) = \Phi_R\left(\Phi^{-1}(u_1), \cdots, \Phi^{-1}(u_n); \theta_c\right) \\ u_j = F_{Xj}\left(x_j\right), \quad j \in [1,n] \end{cases} \tag{30}$$

where θ_c is the covariance matrix, Φ_R is the n-dimensional standard normal distribution function ($\mu = 0, \sigma = 1$), and Φ^{-1} is the inverse function of the one-dimensional standard normal distribution function. Then, the Gaussian copula-constructed TME model can be derived as follows:

$$\begin{cases} FDR(ft_i; S) = 1 - \Phi_R\left(\left\{\Phi^{-1}\left(u_j\right) | j \in [1,n]\right\}; \theta_c\right) \\ u_j = F_{Xj}\left(thr_j\right)^{s_j}, \quad X_j = t_j^i \\ i \in [0,m], \quad j \in [1,n] \end{cases} \tag{31}$$

$$\begin{cases} FIR(ft_i; S) = LI_i^* \cdot \Phi_R\left(\left\{\Phi^{-1}\left(u_j\right) | j \in [1,n]\right\}; \theta_c\right) \\ LI_i^* = \prod_{k=1,k\neq i}^{m} \left(1 - \prod_{j=1}^{n} \left[(1-r_{ij})(1-r_{kj}) + r_{ij}r_{kj}\right]^{s_j}\right) \\ u_j = F_{Xj}\left((-1)^{r_{ij}}\, thr_j\right)^{s_j}, \quad X_j = (-1)^{r_{ij}}\, t_j^i \\ i \in [1,m], \quad j \in [1,n] \end{cases} \tag{32}$$

IV. EFFICACY VALIDATION OF THE DEVELOPED TESTABILITY METRIC ESTIMATION MODEL

To show the accuracy improvement of TME when using the developed model, this section uses two electronic circuits as examples. TME results with both the conventional model and the developed model are compared with statistical TMs. The validation procedure is shown in Fig. 3.

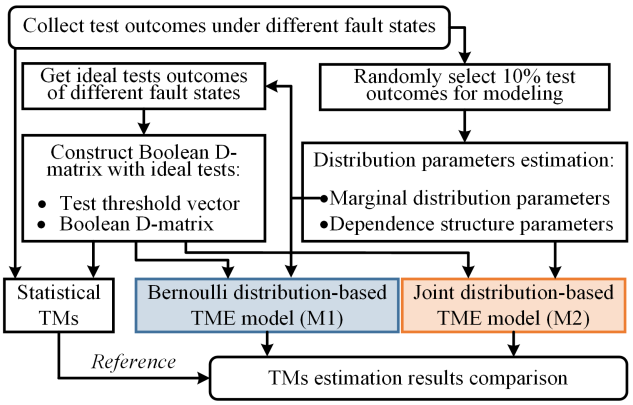

FIGURE 3. Efficacy validation process of the developed TME model.

To generate test outcomes of the circuits, the simulation software PSpice is used. For real applications, the fault seeding experimental data and historical data can also be used. The component tolerance is used as an uncertainty factor of unreliable tests. 10% of all simulation results are randomly selected to estimate distribution parameters, which is used to establish the Boolean D-matrix and two TME models. To establish the Boolean D-matrix, only marginal distributions are needed to extract ideal values of test outcomes. Then, the Boolean D-matrix and corresponding test threshold vector can be obtained. M1 and M2 are used in Fig. 3 to represent two TME models need to be compared, respectively. Besides the information required by the conventional model, dependence structure parameters are also needed for the developed model.

For these two circuits, the test outcomes are pre-confirmed to be dependent so as to induce the dependency issue for TME. Although the distribution parameter estimation errors can also influence TME results, these errors should equally influence both models. Thus, it is fair to say that the dependency among tests is the main factor influencing TME accuracy of these two circuits.

A. TME FOR A LINEAR VOLTAGE DIVIDER

In theory, most complex systems can be simplified using series and/or parallel connections. In analog circuits, the

linear voltage divider is such a circuit that includes both types of connections. Although it is simple, it still possesses the same structural characteristics as complex systems. Thus it is used as an example to validate the developed model.

1) TEST OUTCOMES SIMULATION

The schematic of the linear voltage divider, which includes 10 resistors, is shown in Fig. 4. Five types of faults were simulated (parameter drift faults R_2, R_4, R_6, R_8, and R_{10}), and five tests (referring to the voltage values of the five test points shown in Fig. 4) were considered as candidates. For each resistor, the tolerance was set at 2%, and each fault was simulated by positively shifting 10% of the nominal value of the corresponding resistor. To represent the tolerance influence, 10^3-times simulations were run utilizing the Monte Carlo technique for each fault state.

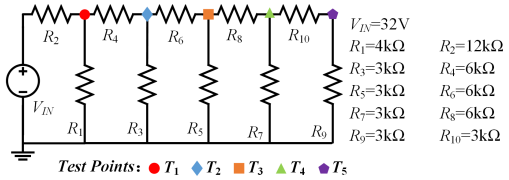

FIGURE 4. Linear voltage divider circuit.

2) BOOLEAN D-MATRIX CONSTRUCTION

Based on the acquired simulation data, the ideal value (mean value) vectors of test outcomes for each fault state can be estimated statistically, as shown in Table 1.

TABLE 1. Ideal values of test outcomes under different faults for the linear voltage divider.

	t_1	t_2	t_3	t_4	t_5
ft_0	16.00	8.00	4.00	2.00	1.00
$ft_1(R_2)$	16.25	8.12	4.06	2.03	1.02
$ft_2(R_4)$	16.13	8.25	4.12	2.06	1.03
$ft_3(R_6)$	16.03	8.06	4.13	2.06	1.03
$ft_4(R_8)$	16.01	8.02	4.03	2.06	1.03
$ft_5(R_{10})$	16.00	8.01	4.02	2.03	1.06

To construct the Boolean D-matrix, test thresholds are needed. In real applications, test thresholds should be determined due to a series of requirements. In this paper, the test threshold is arbitrarily set as the value of $\mu + 3\sigma$ of each test outcome under ft_0, where μ and σ denote the mean value and the standard deviation of the corresponding test outcome. With this criteria, the FAR can be limited at a low level since the majority of test outcomes under ft_0 will be 0 as they are expected. The determined test threshold vector THR is:

$$THR = (16.187, 8.124, 4.072, 2.041, 1.025) \quad (33)$$

Then the test outcome ideal value vector of each fault is compared with THR, respectively. If the ideal value of t_j under ft_i is greater than the corresponding test threshold, t_j is believed to be able to respond to ft_i. Thus, the Boolean D-matrix can be constructed as shown in Table 2.

TABLE 2. Constructed boolean D-matrix for the linear voltage divider.

	t_1	t_2	t_3	t_4	t_5
ft_1	1	1	0	0	0
ft_2	0	1	1	1	1
ft_3	0	0	1	1	1
ft_4	0	0	0	1	1
ft_5	0	0	0	0	1

3) BERNOULLI DISTRIBUTION-BASED TME MODELING

To construct the Bernoulli distribution-based TME model, both the Boolean D-matrix and the marginal distributions of test outcomes are needed.

To estimate the marginal distributions, various estimation algorithms, such as MLE and kernel density estimation, can be used. In this example, the marginal distributions all obey normal distributions well. Hence, mean values and standard deviations can be used to describe these distributions. The mean values of test outcomes are shown in Table 1, and standard deviations are shown in Table 3.

TABLE 3. Standard deviation of each test outcome under different faults.

$\times 10^{-2}$	t_1	t_2	t_3	t_4	t_5
ft_0	0.0621	0.0412	0.0243	0.0137	0.0083
ft_1	0.0565	0.0391	0.0241	0.0137	0.0081
ft_2	0.0618	0.0414	0.0245	0.0141	0.0082
ft_3	0.0655	0.0430	0.0251	0.0140	0.0085
ft_4	0.0605	0.0385	0.0237	0.0138	0.0085
ft_5	0.0634	0.0422	0.0248	0.0140	0.0087

Then, the probabilistic elements d_{ij} in (8) can be calculated, and corresponding TMs can be estimated using (9) and (10).

4) JOINT DISTRIBUTION-BASED TME MODEL

Besides the Boolean D-matrix and the marginal distributions, the construction of the developed TME model also needs dependence parameters of test outcomes. In the copula function, the dependence parameters are called dependence structure parameters.

To estimate the dependence structure parameters in a copula function, first the raw sample data should be transformed, then some general estimation algorithms can be used. Taking the Gaussian copula function as an instance, the raw data should be transformed into the space of $[0, 1]^n$ using $F_{xj}()$. Subsequently, the transformed data should be transformed again using $\Phi^{-1}()$.

Using the data after two-step transformation, the PDF parameters of the following n-dimensional standard normal distribution can be estimated:

$$f_X(x) = (2\pi)^{-\frac{n}{2}} |\rho|^{-\frac{1}{2}} \exp\left(-\frac{1}{2} x^T \rho^{-1} x\right) \quad (34)$$

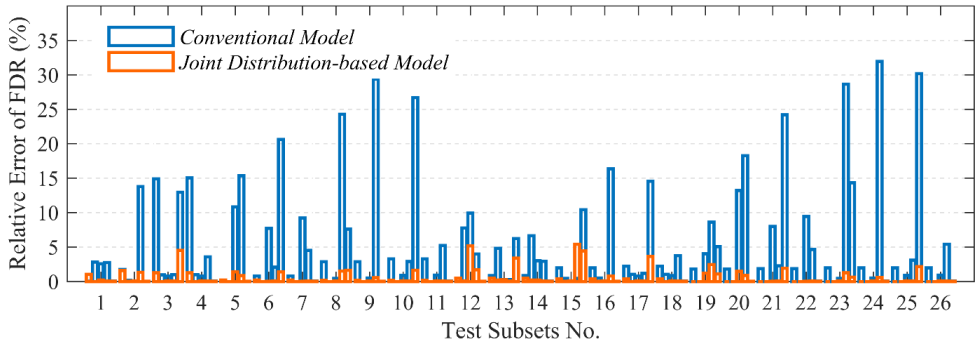

FIGURE 5. Comparison of FDR estimation results for the linear voltage divider using the conventional model vs. the joint distribution-based model.

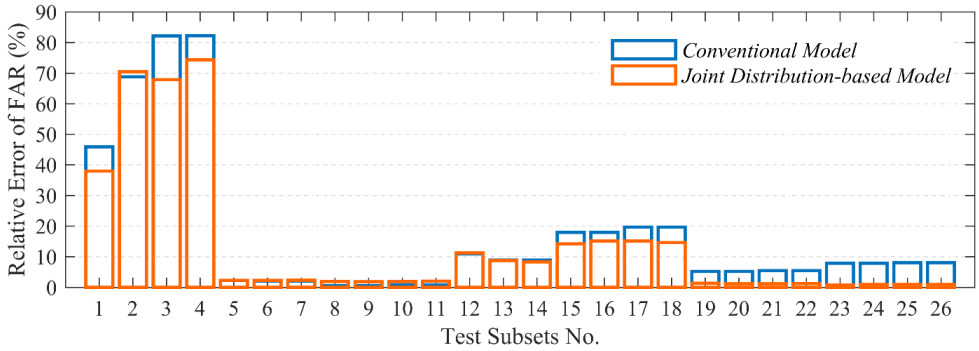

FIGURE 6. Comparison of FAR estimation results for the linear voltage divider using the conventional model vs. the joint distribution-based model.

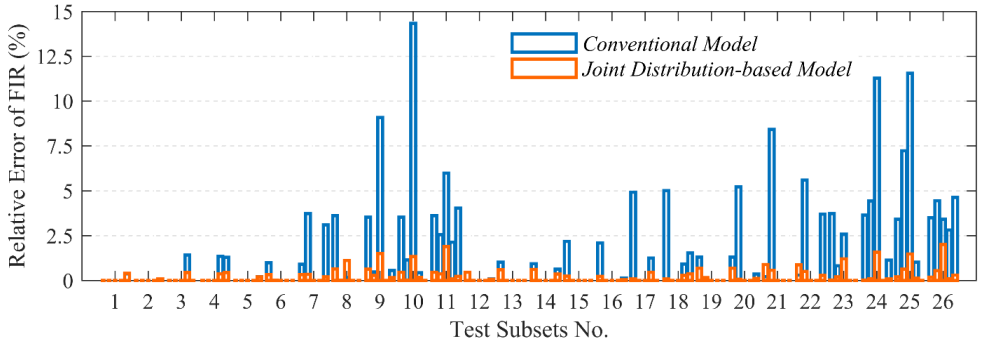

FIGURE 7. Comparison of FIR estimation results for the linear voltage divider using the conventional model vs. the joint distribution-based model.

where X denotes n-dimensional data after transforming and ρ denotes the covariance matrix, which is the structure parameter that needs to be estimated.

Since the test outcomes are transformed, the test thresholds should also be transformed with the same process. Then, the transformed test thresholds can be brought into (31) and (32) for TME. The only thing to note is that during the transforming process for FIR, the item $(-1)^{rij}$ in (32) should be first added to the raw test outcomes and thresholds.

5) TME RESULTS COMPARISON

Using statistical TMs as the reference, the estimation results based on the developed TME model are compared with those of the conventional TME model. To show the improvement of TME better, various test subsets are used. In this example, the total number of non-void subsets is 31. Since test subsets with one single test do not have the dependency problem, they are not considered. Therefore, 26 test subsets are selected, and TME results are shown in Figs. 5–7. Test subsets are sorted from $\{0, 0, 0, 1, 1\}$, $\{0, 0, 1, 0, 1\}$, . . ., to $\{1, 1, 1, 1, 0\}$, $\{1, 1, 1, 1, 1\}$, and are labeled as 1–26. Five bars in each subset group of Fig. 5 and Fig. 7 represent the results for five fault states, respectively. The relative errors (REs) of these 130 conditions coming from two models are listed in Table 4, where M1 represents the conventional TME model and M2 represents the developed TME model.

TABLE 4. TME results comparison for the linear voltage divider.

		ft_0		ft_1		ft_2		ft_3		ft_4		ft_5	
		M1	M2	M1	M2	M1	M2	M1	M2	M1	M2	M1	M2
FDR	Avg. RE%	17.13	13.89	2.76	0.37	1.05	0.02	3.36	0.45	9.10	0.71	6.68	1.02
	Max. RE%	82.23	74.36	15.04	1.57	7.78	0.21	13.21	5.22	31.93	5.32	30.17	4.45
FIR	Avg. RE%	--	--	2.39	0.41	3.16	0.27	7.30	1.51	1.42	0.25	1.45	0.22
	Max. RE%	--	--	5.01	0.89	8.43	0.62	14.34	2.00	2.81	0.46	4.63	0.44

For the FDR, the REs of 33 out of 130 conditions are higher than 5% when M1 is used. Moreover, the REs of 10 out of these 33 conditions are even higher than 10%, and the maximum RE exceeds 31.93%. When M2 is used, only 2 conditions have an RE slightly higher than 5% (5.32% and 5.22%), and the maximum RE decreases to 5.32%. For the FIR, the REs of 33 conditions are higher than 2% when M1 is used. Moreover, the REs of 5 out of these 33 conditions are even higher than 5%, and the maximum RE exceeds 14.34%. When M2 is used, all REs decrease to less than 2%. The average REs of FDR and FIR using M2 are 0.514% and 0.532%, respectively, which are much lower than those of M1 (4.590% and 3.144%, respectively). For the FAR (FDR of ft_0), the average RE decreases from 17.13% to 13.89%. Although the REs of the first 4 test subsets using M2 are higher even than 20%, the absolute errors are all less than 1.0%.

Briefly speaking, the developed model gets higher TME accuracy of the voltage divider than the conventional model, which makes 8.9-fold, 1.2-fold, and 5.9-fold reduction in terms of average TME errors (FDR, FAR, FIR), respectively.

B. TME FOR A NEGATIVE FEEDBACK CIRCUIT

The negative feedback circuit is a basic analog circuit that is widely used for amplifying voltage, current, and power signals in electronic systems.

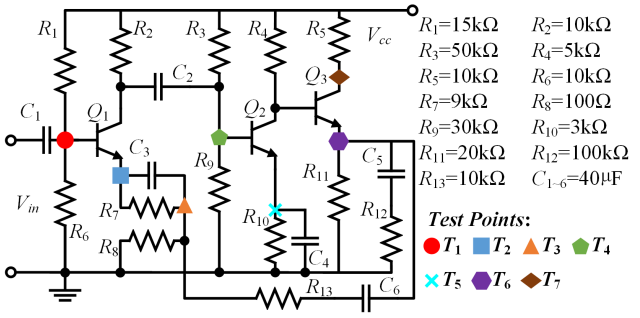

FIGURE 8. Negative feedback circuit.

1) TEST OUTCOMES SIMULATION

A specific multistage negative feedback circuit is shown in Fig. 8. The input signal (V_{in}) is a 1-kHz 7-mV sinusoidal waveform, and V_{cc} is 15 V. Six types of fault (listed in Table 5) were simulated, and DC voltage values of seven test points (pointed out in Fig. 8) were recorded as test outcomes.

TABLE 5. Simulated faults in the negative feedback circuit.

Fault code	Fault mode	Fault code	Fault mode
ft_1	Q_1 B-C short	ft_4	R_8 = 130 Ω
ft_2	Q_1 C-E short	ft_5	R_9 = 39 kΩ
ft_3	Q_2 C-E short	ft_6	R_6 = 13 kΩ

The component tolerance level of resistors was set as 5%. For each fault state, 10^3-times Monte Carlo simulations were run.

TABLE 6. Constructed boolean D-matrix for the negative feedback circuit.

	t_1	t_2	t_3	t_4	t_5	t_6	t_7
ft_1	1	1	1	0	0	0	0
ft_2	0	1	1	0	0	0	0
ft_3	0	0	0	1	1	0	1
ft_4	0	0	1	0	0	0	0
ft_5	0	0	0	1	1	0	0
ft_6	1	1	0	0	0	0	0

2) BOOLEAN D-MATRIX CONSTRUCTION

Following the same procedure as mentioned in Section IV.A, given the test threshold vector in (35), the Boolean D-matrix can be obtained as in Table 6.

$$THR = (6.75, 6.10, 0.07, 5.57, 4.95, 7.76, 12.25) \quad (35)$$

3) CONSTRUCTION OF TWO TME MODELS

For the construction of the conventional TME model and the developed TME model, the process is the same as mentioned in Section IV.A.

4) TME RESULTS COMPARISON

In this example, the total number of subsets including more than one test is 120. Constrained by the figure resolution, it is impossible to put so many results in a single figure. Thus, only subsets including more than four tests are considered in this example. Therefore, TME results of 29 test subsets are shown in Figs. 9-11. Six bars in each subset group of Fig. 9 and Fig. 11 represent the results for six fault states, respectively. The REs coming from two models are listed in Table 7.

For the FDR, the maximum RE decreases from 51.03% to 13.86% when using the developed TME model, and the average RE decreases from 3.06% to 0.76%. For the FAR (FDR of ft_0), the maximum RE decreases from 47.12%

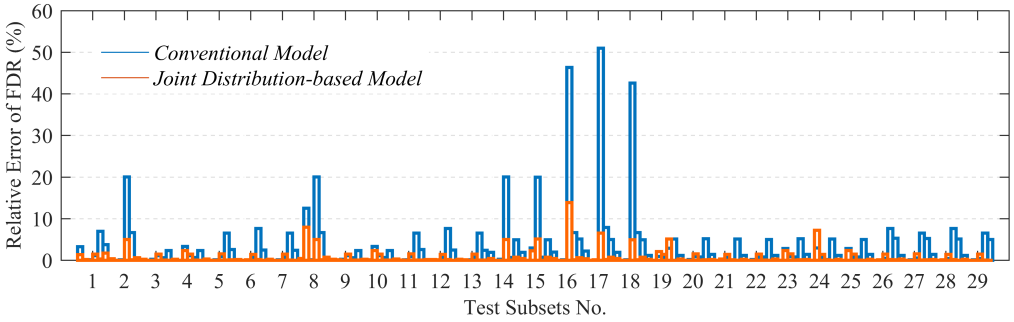

FIGURE 9. Comparison of FDR estimation results for the negative feedback circuit using the conventional model vs. the joint distribution-based model.

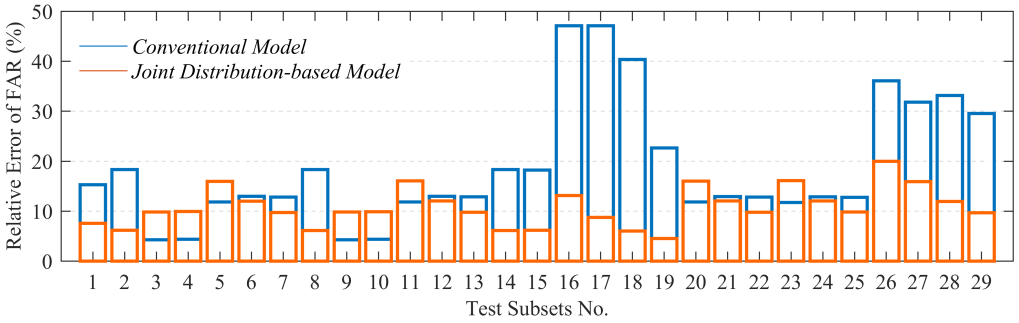

FIGURE 10. Comparison of FAR estimation results for the negative feedback circuit using the conventional model vs. the joint distribution-based model.

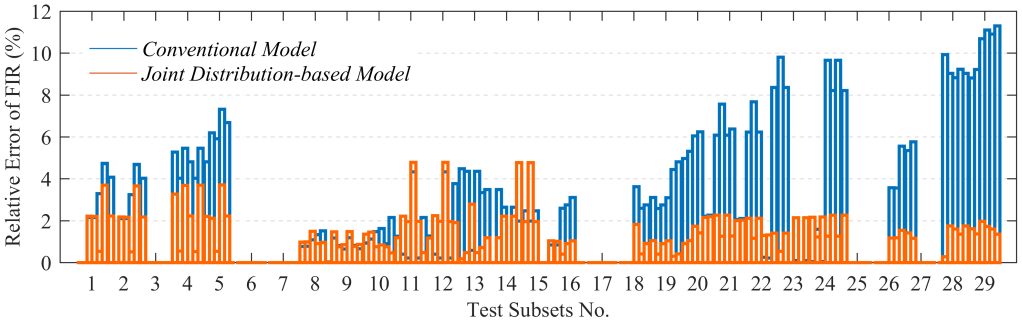

FIGURE 11. Comparison of FIR estimation results for the negative feedback circuit using the conventional model vs. the joint distribution-based model.

TABLE 7. TME results comparison for the negative feedback circuit.

		ft_0		ft_1		ft_2		ft_3		ft_4		ft_5		ft_6	
		M1	M2	M1	M2	M1	M2	M1	M2	M1	M2	M1	M2	M1	M2
FDR	Avg. RE%	18.76	10.79	2.14	0.65	2.50	0.82	2.30	0.51	7.59	1.52	1.55	0.65	2.27	0.40
	Max. RE%	47.12	19.98	20.02	5.01	20.02	7.97	20.03	4.96	51.03	13.86	5.20	7.19	7.66	2.33
FIR	Avg. RE%	--	--	3.19	1.60	0.55	0.55	2.07	1.82	1.73	0.47	4.55	1.62	4.55	0.79
	Max. RE%	--	--	7.33	3.71	1.63	1.50	4.48	4.79	5.32	1.82	9.81	2.27	11.30	1.97

to 19.98%, and the average RE decreases from 18.76% to 10.79%. For the FIR, the maximum RE decreases from 11.30% to 4.79%, and the average RE decreases from 2.77% to 1.14%.

In short, the developed model improves the TME accuracy of the negative feedback circuit, which makes 4-fold, 1.6-fold, and 2.4-fold reduction in terms of average TME errors (FDR, FAR, FIR), respectively.

C. DISCUSSIONS

Although most of the REs using the developed TME model are much lower than the conventional TME model in both examples, there are still several worse results. In Section IV.A, the REs of some test subsets containing only two tests increase slightly after using the developed TME model. This situation occurs when certain test outcomes have a weak dependent relationship between each other and errors from marginal distribution estimation and Monte Carlo sampling dominate the estimation errors. For large errors coming from the FAR estimation, it is mainly caused by the relatively small value of real FAR. On the other hand, the estimation results for the negative feedback circuit are higher than those for the linear voltage divider. As the test dimension increases, the distribution parameters estimation errors also increase.

Nevertheless, the estimation errors using the developed TME model are still within reasonable limits and can be further refined by increasing sample numbers, improving the estimation confidence of marginal distributions and dependence structure parameters, and introducing another type of copula function.

V. CONCLUSIONS

Unreliable tests can significantly influence the testability metric estimation (TME) for complex systems. The only TME model for unreliable tests using Bernoulli distributions adopted an impractical assumption that test outcomes are independent. Therefore, it is ineffective since test outcomes are always dependent. This paper developed a TME model with the joint distribution constructed by the copula theory to eliminate the impractical independent assumption in the conventional model.

In the paper, test outcomes were first proved to be dependent in many cases. Any factor that can simultaneously cause variations of two (or more) test outcomes makes these test outcomes dependent. Such factors include but are not limited to the test equipment error, the fluctuation of environmental conditions, and component tolerances in the system. The joint distribution was then first used for TME. Compared with the Bernoulli distribution-based TME model for unreliable tests, the developed TME model using the joint distribution can quantify the dependent relationships among test outcomes. Thus, the developed TME model can be adopted in any application no matter whether the test outcomes are independent or not. Specifically, a joint distribution construction method—the copula—was also used, which is effective even if a different type of marginal distribution is needed for each test outcome.

The efficacy of the developed model was verified using two electronic circuits with dependency among test outcomes. Testability metrics (including FDR, FAR, and FIR) were estimated using both the conventional and the developed model. For the linear voltage divider, the developed model made 8.9-fold, 1.2-fold, and 5.9-fold improvements of TME accuracy, respectively, when compared with the conventional model. For the negative feedback circuit, the developed model also made 4-fold, 1.6-fold, and 2.4-fold improvements of TME accuracy, respectively. The comparison results showed the conventional model is incorrect when test outcomes are dependent, whereas the developed model can correctly estimate testability metrics.

TME is not only important for the test selection in the design phase, but also necessary for the testability validation in the demonstration phase and the test sequencing in the fault diagnosis phase. The developed TME model can also be extended to these problems. On the other hand, by setting multiple thresholds, the developed model can be further extended to multi-outcome issues.

REFERENCES

[1] S. Chessa and P. Santi, "Comparison-based system-level fault diagnosis in ad hoc networks," in *Proc. 20th IEEE Symp. Rel. Distrib. Syst.*, Oct. 2001, pp. 257–266.

[2] J. W. Sheppard and S. G. W. Butcher, "A formal analysis of fault diagnosis with *D*-matrices," *J. Electron. Test.*, vol. 23, no. 4, pp. 309–322, Aug. 2007.

[3] S. Singh, S. W. Holland, and P. Bandyopadhyay, "Trends in the development of system-level fault dependency matrices," in *Proc. IEEE Aerosp. Conf.*, Big Sky, MT, USA, Sep. 2010, pp. 1–9.

[4] J. A. Starzyk, D. Liu, Z.-H. Liu, D. E. Nelson, and J. O. Rutkowski, "Entropy-based optimum test points selection for analog fault dictionary techniques," *IEEE Trans. Instrum. Meas.*, vol. 53, no. 3, pp. 754–761, Jun. 2004.

[5] V. C. Prasad and N. S. C. Babu, "Selection of test nodes for analog fault diagnosis in dictionary approach," *IEEE Trans. Instrum. Meas.*, vol. 49, no. 6, pp. 1289–1297, Dec. 2000.

[6] S. Zhang, K. R. Pattipati, Z. Hu, and X. Wen, "Optimal selection of imperfect tests for fault detection and isolation," *IEEE Trans. Syst., Man, Cybern., Syst.*, vol. 43, no. 6, pp. 1370–1384, Nov. 2013.

[7] R. DePaul, "Logic modeling as a tool for testability," in *Proc. AUTOTESTCON Symp.*, 1985, pp. 203–207.

[8] J. W. Sheppard and W. R. Simpson, "Applying testability analysis for integrated diagnostics," *IEEE Design Test Comput.*, vol. 9, no. 3, pp. 65–78, Sep. 1992.

[9] S. Deb, K. R. Pattipati, V. Raghavan, M. Shakeri, and R. Shrestha, "Multi-signal flow graphs: A novel approach for system testability analysis and fault diagnosis," *IEEE Aerosp. Electron. Syst. Mag.*, vol. 10, no. 5, pp. 14–25, May 1995.

[10] G. Zhang, "Optimum sensor localization/selection in a diagnostic/prognostic architecture," Ph.D. dissertation, Dept. Elect. Comput. Eng., Georgia Inst. Technol., Atlanta, GA, USA, 2005.

[11] Y. Cui, J. Shi, and Z. Wang, "An analytical model of electronic fault diagnosis on extension of the dependency theory," *Rel. Eng. Syst. Saf.*, vol. 133, pp. 192–202, Jan. 2015.

[12] S. Sen, S. S. Nath, V. N. Malepati, and K. R. Pattipati, "Simulation-based testability analysis and fault diagnosis," in *Proc. AUTOTESTCON*, Dayton, OH, USA, 1996, pp. 136–148.

[13] X. Tang, A. Xu, R. Li, M. Zhu, and J. Dai, "Simulation-based diagnostic model for automatic testability analysis of analog circuits," *IEEE Trans. Comput.-Aided Design Integr. Circuits Syst.*, vol. 37, no. 7, pp. 1483–1493, Jul. 2018.

[14] T. Golonek and J. Rutkowski, "Genetic-algorithm-based method for optimal analog test points selection," *IEEE Trans. Circuits Syst., II, Exp. Briefs*, vol. 54, no. 2, pp. 117–121, Feb. 2007.

[15] C. Yang, S. Tian, and B. Long, "Application of heuristic graph search to test-point selection for analog fault dictionary techniques," *IEEE Trans. Instrum. Meas.*, vol. 58, no. 7, pp. 2145–2158, Jul. 2009.

[16] R. Jiang, H. Wang, S. Tian, and B. Long, "Multidimensional fitness function DPSO algorithm for analog test point selection," *IEEE Trans. Instrum. Meas.*, vol. 59, no. 6, pp. 1634–1641, Jun. 2010.

[17] C. Yang, S. Tian, B. Long, and F. Chen, "Methods of handling the tolerance and test-point selection problem for analog-circuit fault diagnosis," *IEEE Trans. Instrum. Meas.*, vol. 60, no. 1, pp. 176–185, Jan. 2011.

[18] X. Tang, A. Xu, and S. Niu, "KKCV-GA-based method for optimal analog test point selection," *IEEE Trans. Instrum. Meas.*, vol. 66, no. 1, pp. 24–32, Jan. 2017.
[19] K. R. Pattipati and M. G. Alexandridis, "Application of heuristic search and information theory to sequential fault diagnosis," *IEEE Trans. Syst., Man, Cybern.*, vol. 20, no. 4, pp. 872–887, Jul. 1990.
[20] J. A. Nachlas, S. R. Loney, and B. A. Binney, "Diagnostic-strategy selection for series systems," *IEEE Trans. Rel.*, vol. 39, no. 3, pp. 273–280, Aug. 1990.
[21] V. Raghavan, M. Shakeri, and K. Pattipati, "Test sequencing algorithms with unreliable tests," *IEEE Trans. Syst., Man, Cybern. A, Syst. Humans*, vol. 29, no. 4, pp. 347–357, Jul. 1999.
[22] J. Ying, T. Kirubarajan, K. R. Pattipati, and A. Patterson-Hine, "A hidden Markov model-based algorithm for fault diagnosis with partial and imperfect tests," *IEEE Trans. Syst., Man, Cybern. C, Appl. Rev.*, vol. 30, no. 4, pp. 463–473, Nov. 2000.
[23] S. Ruan, Y. Zhou, F. Yu, K. P. Pattipati, P. Willett, and A. Patterson-Hine, "Dynamic multiple-fault diagnosis with imperfect tests," *IEEE Trans. Syst., Man, Cybern. A, Syst. Humans*, vol. 39, no. 6, pp. 1224–1236, Nov. 2009.
[24] S.-G. Zhang, Z. Hu, and X.-S. Wen, "Sequential fault diagnosis strategy with imperfect tests considering life cycle cost," *J. Central South Univ.*, vol. 20, no. 12, pp. 3513–3521, Dec. 2013.
[25] C. Yang, F. Chen, and S. Tian, "Grouped genetic algorithm based optimal tests selection for system with multiple operation modes," *J. Electron. Test.*, vol. 33, no. 4, pp. 415–429, Aug. 2017.
[26] C. Zhao, K. P. Pattipati, G. Liu, J. Qiu, K. Lv, and T. Li, "A Markov chain-based testability growth model with a cost-benefit function," *IEEE Trans. Syst., Man, Cybern. Syst.*, vol. 46, no. 4, pp. 524–534, Apr. 2016.
[27] C. Zhao, J. Qiu, G. Liu, and K. Lv, "Planning, tracking and projecting method for testability growth based on in time correction," *Proc. Inst. Mech. Eng. O, J. Risk Rel.*, vol. 230, no. 2, pp. 228–236, Feb. 2016.
[28] Z. Zhao, Y. Zhang, G. Liu, and J. Qiu, "Statistical analysis of time-varying characteristics of testability index based on NHPP," *IEEE Access*, vol. 5, pp. 4759–4768, 2017.
[29] C. Jiang, W. Zhang, B. Wang, and X. Han, "Structural reliability analysis using a copula-function-based evidence theory model," *Comput. Struct.*, vol. 143, pp. 19–31, Sep. 2014.
[30] P. Jaworski, F. Durante, W. F. Härdle, and T. Rychlik, *Copula Theory and Its Applications*. New York, NY, USA: Springer, 2010.

XUERONG YE (M'11–SM'18) received the B.S., M.S., and Ph.D. degrees in electrical engineering from the Harbin Institute of Technology, Harbin, China, in 2003, 2005, and 2009 respectively. He is currently an Associate Professor with the Department of Electrical Engineering, Harbin Institute of Technology. His research interests include failure analysis, and reliability design for electronic devices and systems.

CEN CHEN (S'15) was born in 1992. He received the B.S. degree in electrical engineering from the Harbin Institute of Technology, Harbin, China, in 2014, where he is currently pursuing the Ph.D. degree.

Since 2017, he has been a Visiting Research Scholar with the Center for Advanced Life Cycle Engineering, University of Maryland at College Park, College Park, MD, USA. His research interests include testability design techniques for power electronics, accelerated degradation test, condition monitoring, fault diagnosis, and prognosis for power electronic components.

MYEONGSU KANG (M'17) received the B.E. and M.S. degrees in computer engineering and information technology and the Ph.D. degree in electrical, electronics, and computer engineering from the University of Ulsan, Ulsan, South Korea, in 2008, 2010, and 2015, respectively. He is currently a Research Scientist with the Center for Advanced Life Cycle Engineering, University of Maryland at College Park, College Park, MD, USA. His current research interests include data-driven anomaly detection, diagnostics, and prognostics of complex systems, such as automotive, railway transportation, and avionics, for which failure would be catastrophic. He has expertise in analytics, machine learning, system modeling, and statistics for prognostics and systems health management.

GUOFU ZHAI (M'06) received the Ph.D. degree from the Harbin Institute of Technology, Harbin, China, in 1998. He is currently a Professor with the Department of Electrical Engineering, Harbin Institute of Technology. He has published over 40 peer-reviewed journal papers. His research interests include the reliability and testing techniques of electronic devices and systems.

MICHAEL PECHT (F'92) received the B.S. degree in physics in 1976, the M.S. degree in electrical engineering in 1978, and the M.S. and Ph.D. degrees in engineering mechanics from the University of Wisconsin–Madison, USA, in 1979 and 1982, respectively.

He is currently the Founder and the Director of the Center for Advanced Life Cycle Engineering, University of Maryland at College Park, College Park, MD, USA, which is funded by over 150 of the world's leading electronics companies at over US$ 6 million/year. He is also a Chair Professor of mechanical engineering and a Professor of applied mathematics, statistics, and scientific computation with the University of Maryland. He has written over 20 books, 400 technical articles, and has eight patents.

Dr. Pecht is a Professional Engineer, and a fellow of the American Society of Mechanical Engineers, the Society of Automotive Engineers, and the International Microelectronics Assembly and Packaging Society. He has also served on three U.S. National Academy of Science Studies, two U.S. Congressional Investigations in automotive safety, and as an Expert to the U.S. Food and Drug Administration. He is the Editor-in-Chief of the IEEE ACCESS, and served as the Chief Editor for the IEEE TRANSACTIONS ON RELIABILITY for nine years and *Microelectronics Reliability* for 16 years.